Maximum Power Point Tracking Strategies of Grid-Connected Wind Energy Conversion Systems

Ali M. Eltamaly, Mohamed A. Mohamed, and Ahmed G. Abo-Khalil

Abstract In order to achieve maximum power point tracking (MPPT) of wind energy systems, the rotating speed of wind turbines (WTs) ought to be adjusted in the constant as indicated by wind speeds. However, fast wind speed varieties and heavy inertia bargain the MPPT control of WTs. This chapter proposes a fuzzy logic controller (FLC)-based MPPT strategy for Wind Energy Conversion Systems (WECS). The performance of the proposed MPPT strategy is analyzed mathematically and verified by simulation using MATLAB/PSIM/Simulink software. The proposed method improves the speed and accuracy of MPPT. Furthermore, the simulation results have been conducted to approve the performance of the proposed MPPT strategy, and all results have confirmed the adequacy of the proposed MPPT strategy.

Keywords Maximum power point tracking (MPPT) · Wind energy conversion systems (WECS) · Fuzzy logic controller (FLC) · Wind turbine (WT)

A. M. Eltamaly (✉)
Faculty of Engineering, Electrical Engineering Department, Mansoura University, Mansoura 35511, Egypt
e-mail: eltamaly@ksu.edu.sa

Sustainable Energy Technologies Center, King Saud University, Riyadh 11421, Saudi Arabia

K.A. CARE Energy Research and Innovation Center, Riyadh 11451, Saudi Arabia

M. A. Mohamed
Faculty of Engineering, Electrical Engineering Department, Minia University, Minia 61519, Egypt

A. G. Abo-Khalil
Department of Electrical Engineering, College of Engineering, Majmaah University, Almajmaah 11952, Saudi Arabia

Department of Electrical Engineering, College of Engineering, Assiut University, Assiut 71515, Egypt

1 Introduction

The energy of the wind has played a major role in the energy systems since time immemorial especially as a windmill in producing mechanical power [1–4]. In the last century, wind energy found application in electricity generation using wind turbines (WTs) technology [5–7]. The total installed wind power capacity of the world was estimated at 539 GW in 2017 where 52.6 added in 2017 as found in the 2017 world energy report of the world wind energy association. This installed capacity has the potential to produce 944 Terawatt-hours annually (TWh/year) and accounts for 5% of worldwide electricity consumption [8]. Annual growth rates of cumulative wind power capacity have averaged 10.8% since the end of 2016, and global capacity has increased eightfold over the past decade. Figure 1 shows the top 10 countries by nameplate wind power capacity at the end of 2017 [9–11]. For the generation of energy through the wind, WTs are used, which consist basically of blades (collectors of the kinetic energy of the wind), in addition to two axes (low and high speed), the low speed being connected to a multiplier of wind speed and the high-speed connection to the generator. The current wind systems also use a series of electronic devices aimed at controlling and acting on the energy supply of the turbines, such as power converters and "soft-starters", thus realizing the interface between the generator and the electrical network.

WTs operate at wind speed values between 5 and 25 m/s (average speed). At values below 5 m/s the turbines are unable to deliver power to the system, while for winds well above 25 m/s the turbines must not operate for safety reasons due to mechanical resistance limits. For slightly higher speed values rated, the turbines
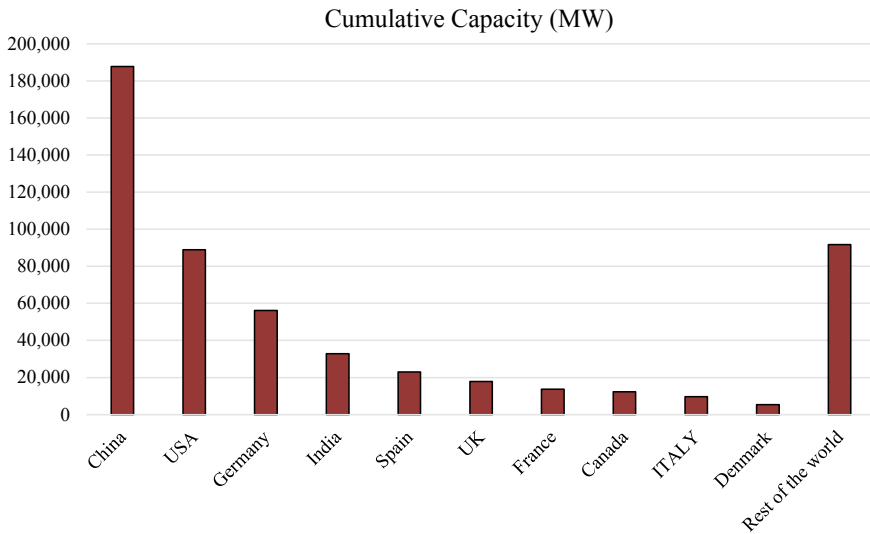
Fig. 1 Top 10 countries by nameplate wind power capacity at the end of 2017

must have control systems that reduce the use of wind energy by changing the angle of the blades in relation to the winds, thus maintaining constant power.

Typical speed values or blade tips range from 60 to 100 m/s, thus generating power between 5–10 and 2–3 MW. If connected to the grid, it is necessary to generate power with the rotor operating at a typical rotation for a frequency of 60 Hz or 50 Hz. There are two basic ways of operating wind systems:

– *Turbine operating at fixed speed*

Fixed speed wind turbines are relatively simple, consisting of a low-speed rotor rotating by the action of the winds on the turbine blades, speed multiplier, and high-speed rotor connected to the generator. These were, historically, the first to be commercially implemented.

Squirrel cage induction generators are typically used due to their simplicity. As in this type of turbine the operating speed varies very little, less than 1%, the slip of the generator varies very little too. Capacitors are usually connected in parallel with the supply circuit to correct the generator's power factor since this being an induction machine, it consumes reactive energy. "Soft-starters" must also be used to obtain a smooth growth of the magnetic flux and the electric current at the initial moment of energizing the generating unit.

– *Turbine operating at variable speed*

Nowadays it is more common to use it in large wind systems connected to the electric power networks, because over time, the size and power of the wind farms increased, thus leading to a migration of the technology of generators working at a fixed speed to variable speed. The main advantages of this technology are that it allows the connection of these generators to large electric power networks, in addition to being viable for the generation of high energy values, in addition to being used in certain cases that do not use the speed multiplier.

There are broadly two commercially existing WTs technologies namely the horizontal axis (HA-WT) and the vertical axis (VA-WT) [12–16] as detailed in the following sections. The HA-WT type has from one to three rotor blades usually directed at the wind thus the rotor has fastened tail-vanes to continuously position the blades in the path of the wind. The VA-WT type is not required to be aimed at the wind and works independently of the direction of the wind. The vertical WT however, requires more ground space because of its vertical structure [17]. WTs are often mounted on vertical structures known as towers above the ground.

1.1 Horizontal Axis WTs (HA-WTs)

This is the most renowned type of WTs. There are many designs for this type, which are shown in Fig. 2. Modern HA-WTs characteristically use two or three blades. Most European WTs are three-bladed designs [18–20]. Two-bladed designs of WTs
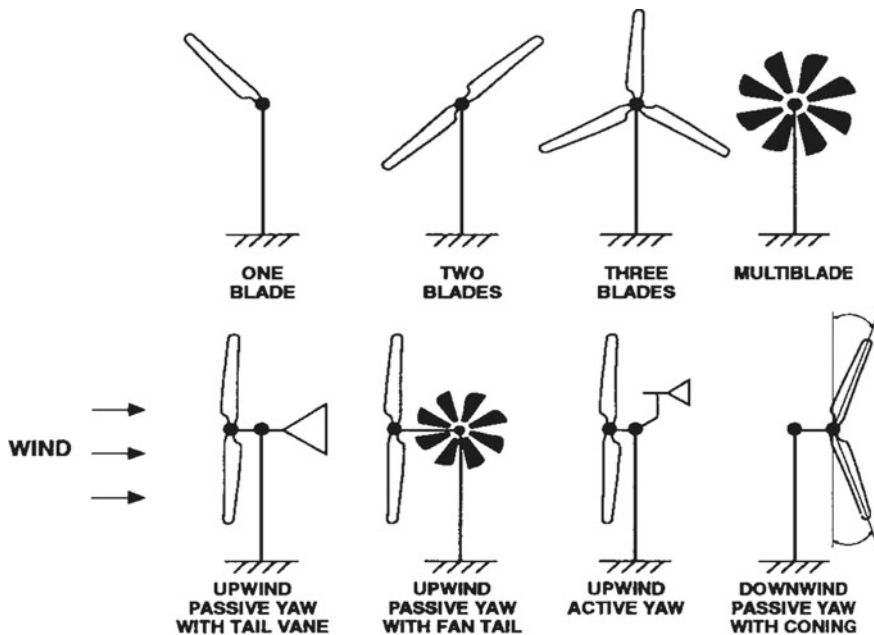
Fig. 2 HA-WT configurations

have the advantage of reducing the cost of one rotor blade and its weight. However, they require a higher rotational speed to produce the same energy output. Lately, several traditional manufacturers of two-bladed machines have switched to three-bladed machines. A one-bladed wind turbine is also possible; however, it is not very widespread commercially, due to the same problems of two-bladed design applied to one-bladed machines. In addition to higher rotational speed, they produce noise in the process of rotating the counterweight of the rotor placed on the other side of the hub from the rotor blade to balance the rotor [21–25].

Figure 3 shows the influence of the number of blades on the rotor power coefficient [26]. It is obvious from this figure that three-bladed HA-WTs have the maximum obtainable power coefficient and it works at optimal tip speed ratio. The tip speed ratio is the ratio between the tangential speed of the tip of a blade and the actual velocity of the wind [27, 28]. The noise produced by a WT is proportional to the tip speed ratio. So, the three-bladed design has lower noise which makes it the most attractive option. Also, higher tip speed ratio WTs need stronger blades to compensate for the higher centrifugal forces [29, 30].

As shown in Fig. 3, the power coefficient increases slightly with the increasing number of blades. As a result, a compromising between the increases in the power generated and the cost of extra blades should be done [32]. Most of the European manufacturers prefer three-bladed design for more stability and lesser noise while most of the USA manufacturers prefer the two-bladed design to save the cost of
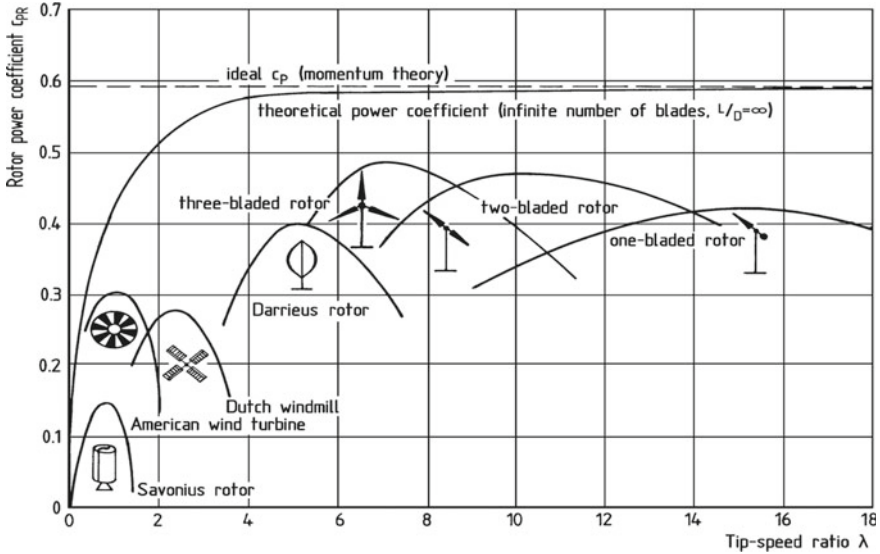
Fig. 3 Influence of the number of blades on the rotor power coefficient (envelope) and the optimum tip speed ratio [31]

one extra blade with the argument that the increase in the generation from two to three-bladed design will not compensate for the cost of the extra blade [33]. Due to the high noise associated with two-bladed design, the requirement for stronger blades, the need for high wind speed sites, and the lower power coefficient make the two-bladed design less attractive. However, the two-bladed design may be attractive also in high wind speed sites and offshore applications. The main advantages of HA-WTs are self-starting, a large variety of the rated output power (Suitable for small WTs as well as very large WTs), and comparatively low cost [34–37].

There are two main disadvantages to this type. The first is the requirement that the complete components (such as generator, gearbox, and control system) of the HA-WT be located at the top of the WT which makes maintenance difficult at such heights [38]. Secondly, when the wind changes direction, the HA-WT should be reoriented to be aligned with the change in direction [39, 40].

1. *Upwind and Downwind Horizontal Axis WTs*

Upwind WTs have the rotor facing the wind to make the wind hit the blades before the tower as shown in Fig. 4a [41–45]. This technique has the following features:

- Remedy the problem of spikes on the WT's output voltage due to the wind shade that the tower causes when the blades move in front of the tower especially in constant speed systems.
- It decreases the power fluctuations.
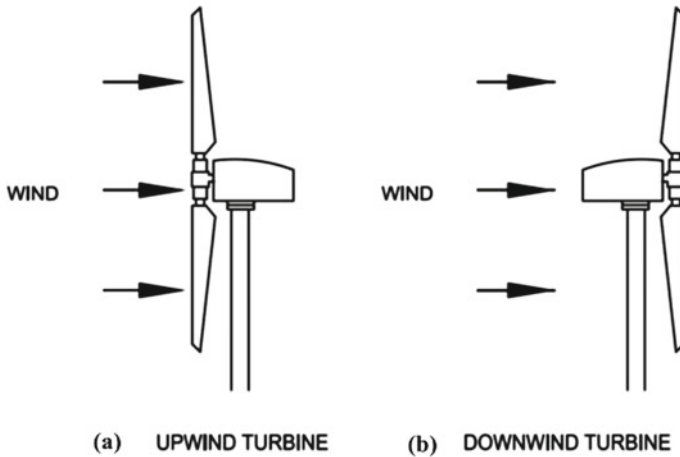
Fig. 4 Wind direction facing the wind turbine generator

- Because the blades can hit the tower it requires a rigid hub with rigid blades away from the tower to avoid touching the tower.
- This design is prominent in very large scale WTs.

Downwind WTs have the rotor on the flow-side as shown in Fig. 4b. This configuration is paramount in small and medium-size WTs. This configuration may not need a yaw mechanism if it is equipped with the streamlined body in the nacelle that will make it follow the wind [46–49]. It has the following features:

- The rotor blades are more flexible as they can bend away from the tower.
- It does not require a rigid tower as in the case of upwind.
- It suffers from the variation in output voltage and power due to the effect of the wind shadow caused by the tower.

1.2   Vertical Axis WTs (VA-WTs)

VA-WTs type is less available as compared to the HA-WTs as a result of some design constraints. In addition to the VA-WTs having a narrow range of rated output power, it also requires a starting motor and has a high comparative cost [50–52]. The main advantages of VA-WTs, are that; no additional cost is required to change the VA-WTs direction when the wind direction changes and the gearbox, generator, and control system are at the ground level thus making maintenance is very simple. Figure 5 shows different VA-WTs configurations.
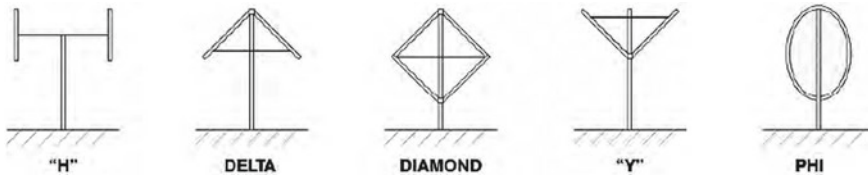
Fig. 5 VA-WTs configurations [51]

1.3 Wind Resource

Wind resources are categorized into wind regimes according to the mean speeds of the sites. To install small wind turbines of less than 100 kW, annual mean wind speeds of 4.0–4.5 m/s (14.4–16.2 km/h; 9.0–10.2 mph) are required to make the system cost-effective [53]. The wind energy conversion system (WECS) most often referred to as the WT for short should be decided upon only after assessing the site wind resources. The most important data is hourly mean wind speed taken over for at least twelve months. Many years' data will provide a more accurate estimation of the annual mean wind speed of the site [54].

All nations have national meteorological administrations that record and distribute climate-related information, including wind paces and headings. The strategies are settled and composed inside the World Meteorological Association in Geneva, with the principle point of giving constant runs of information for a long time. Information have a tendency to be recorded at a moderately few for all time staffed official stations utilizing strong and confided in gear. Sadly, for wind control forecast, official estimations of wind speed tend to be estimated just at the one standard stature of 10 m, also, at stations close to airplane terminals or towns where protection from the breeze might be a characteristic component of the site. Such information are, in any case, critical as fundamental "stays" for automated breeze displaying, yet are not appropriate to apply straightforwardly to foresee wind control conditions at a particular site. Standard meteorological breeze information from the closest authority station are just valuable as first-arrange gauges; they are not adequate for definite arranging, particularly in sloping (complex) landscape. Estimations at the designated site at a few statures are expected to foresee the power created by specific turbines. Such estimations, notwithstanding for a couple of months yet best for a year, are contrasted and standard meteorological information so that the fleeting correlation might be utilized for longer term expectation; the strategy is called "measure-connect foresee". Also, data is held at expert breeze control information banks that are gotten from air ship estimations, wind control establishments and scientific demonstrating, and so forth. Such composed and open data is progressively accessible on the Internet. Wind control forecast models empower point by point wind control forecast for forthcoming breeze turbine destinations from moderately meager nearby information, even in uneven territory [54, 55].

2 Wind Energy Conversion Systems (WECS)

WT can be one of the renewable energy components of the HRES. WTs are classified from several viewpoints as discussed before. From the rotational speed perspective, there is fixed speed (FS), limited variable speed (LVS), and variable speed (VS) WTs. From the power regulation perspective WTs are classified into stall and pitch control. From the side of drive train WT is grouped into direct drive (DD) and gear drive (GD). The FS type uses a gearbox, squirrel cage induction generator (SCIG), and classified as stall, active stall, and pitch control WT. Most of the HRES are using a small WT size lower than 250 kW that may use PMSG with DC or AC output power [55, 56]. The integration configuration of the WTs depends on the output voltage type (AC or DC) as will be discussed below.

WTs can be classified according to the rotational speed concept, variable, and constant rotational speed. The variable speed operation has many advantages over constant speed operation such as increased energy capture, operation at MPPT over a wide range of wind speeds, high power quality, reduced mechanical stresses, aerodynamic noise improved system reliability, and it can provide (10–15%) higher output power and has less mechanical stresses in comparison with the operation at a fixed speed [57]. Also, WTs can be classified according to the type of drive train into direct drive (DD) and gear drive (GD). The DD operation WTs have no gearbox and have been used with small and medium-size WTs employing permanent magnet synchronous generator (PMSG) with higher numbers of poles to eliminate the need for gearbox which can be translated to higher efficiency. The GD type uses a gearbox, squirrel cage induction generator (SCIG), and classified as stall, active stall, and pitch control WT and work in constant speed applications. The variable speed WT uses doubly-fed induction generator, (DFIG) especially in high rating WTs. PMSG appears more and more attractive, because of the advantages of permanent magnet, (PM) machines over electrically excited machines such as its higher efficiency, higher energy yield, no additional power supply for the magnet field excitation, and higher reliability due to the absence of mechanical components such as slip rings. Besides, the performance of PM materials is improving, and the cost is decreasing in recent years. Therefore, these advantages make direct drive PM WT systems more attractive in the application of small and medium-scale WTs [57].

The robust controller has been developed in many literature [58–60] to track the MP available in the wind. They include tip speed ratio (TSR) [61], power signal feedback (PSF) [62], and the hill-climb searching (HCS) [59] methods. The TSR control method regulates the rotational speed of the generator to maintain an optimal TSR at which power extracted is maximum [61]. For TSR calculation, both the wind speed and turbine speed need to be measured, and the optimal TSR must be given to the controller. The first barrier to implement TSR control is the wind speed measurement, which adds to system cost and presents difficulties in practical implementations. The second barrier is the need to obtain the optimal value of TSR, this value is different from one system to another. This depends on the turbine generator characteristics results in custom-designed control software tailored for individual

WTs. In PSF control [62], it is required to have the knowledge of the wind turbine's MP curve, and track this curve through its control mechanisms. The power curves need to be obtained via simulations or offline experiments on individual WTs or from the datasheet of WT which makes it difficult to implement with accuracy in practical applications [63]. The HCS technique does not require the data of wind, generator speeds, and turbine characteristics. But, this method works well only for very small WT inertia. For large inertia WTs, the system output power is interlaced with the turbine mechanical power and rate of change in the mechanically stored energy, which often renders the HCS method ineffective [59]. On the other hand, different algorithms have been used for MP extraction from WT in addition to the three methods mentioned above. For example, reference [55] presents an algorithm for MP extraction and reactive power control of an inverter through the power angle, δ of the inverter terminal voltage, and the modulation index, m_a based variable speed WT without a wind speed sensor. Reference [64] presents an algorithm for MPPT via controlling the generator torque through q-axis current and hence controlling the generator speed with a variation of the wind speed. These techniques are used for a decoupled control of the active and reactive power from the WT through q-axis and d-axis current individually. Also, reference [65] presents a decoupled control of the active and reactive power from the WT, independently through q-axis and d-axis current but MPP operation of turbine system has been produced through regulating the input dc current of the dc/dc boost converter to follow the optimized current reference [65]. Reference [66] presents an algorithm for MPPT through directly adjusting DR of the dc/dc boost converter and modulation index of the PWM–VSC. Reference [67] presents the MPPT control algorithm based on measuring the dc-link voltage and current of the uncontrolled rectifier to attain the maximum available power from wind. Finally, references [68, 69] present MPPT control based on a fuzzy logic control (FLC). The function of FLC is to track the generator speed with the reference speed for MP extraction at variable speeds. The MPPT algorithms can be divided into two categories, the first one is MPPT algorithms for WT with wind speed sensor and the second one is MPPT algorithms without a wind speed sensor (sensorless MPPT controller). The wind speed sensor is normally used in conventional wind energy conversion systems, WECS for implementing the MPPT control algorithm. This algorithm increases cost and reduces the reliability of the WECS in addition to inaccuracies in measuring the wind speed. Therefore, some MPPT control methods estimate the wind speed; however, many of them require the knowledge of air density and mechanical parameters of the WECS [57]. Such methods require turbine generator characteristics that result in custom-design software tailored for individual WTs. Air density, on the other hand, depends upon climatic conditions and may vary considerably over various seasons. Therefore, this technique is not favorite in the modern design of WT and a lot of research efforts are focused on developing wind speed sensorless MPPT controller which does not require the knowledge of air density and turbine mechanical parameters. Therefore, the cost and maintenance of the power control system are decreased and implementation of the power control system is not difficult compared to the sensor MPPT controller [70].

According to [71], only a portion of the kinetic energy of the wind that reaches the area of the turbine blades is converted into the rotational energy of the rotor. This conversion of part of the kinetic energy of the winds causes a reduction in its speed right after it passes through the blades of the wind turbine. If we try to extract all the kinetic energy from the incident wind, the air would end at zero speed, that is, the air could not leave the turbine. In this case, we would not be able to extract energy, since obviously all the air would also be prevented from entering the turbine rotor. In the other extreme case, the wind speed after passing through the blades would remain the same as the speed before passing. With that, we would not have extracted energy from the wind either.

It is possible to assume that there must be some form of a reduction in the speed of the wind that is between these two extremes and is the most efficient situation to convert the kinetic energy of the winds into rotational energy in the rotor. According to [71], the answer is to reduce the wind at the turbine output to 2/3 of its original speed. This ideal operating point is known as Betz's Law, whose main result says that the maximum portion of the kinetic energy of the wind that can be converted into mechanical energy by a wind turbine is 59% [72].

The portion of the wind power converted into rotational energy of the rotor and which will be transmitted to the electric generator through the gear system is then defined by multiplying the power coefficient by the total wind power:

$$P_m = \frac{1}{2} C_P(\lambda, \beta) \, \rho \, A \, u^3 \tag{1}$$

where,

C_p Turbine power coefficient.
ρ Air density (kg/m^3).
A Turbine sweeping area (m^2).
u wind speed (m/s).
λ tip speed ratio of the WT which is given by the following equation [57];

$$\lambda = \frac{r_m \, \omega_r}{u} \tag{2}$$

where, r_m is the turbine rotor radius, ω_r is the angular velocity of the turbine (rad/s).

The turbine power coefficient, C_p, describes the power extraction efficiency of the WT. It is a nonlinear function of both tip speed ratio, λ, and the blade pitch angle, β. While its maximum theoretical value is approximately 0.59, it is practically between 0.4 and 0.45. There are many different versions of fitted equations for C_p made in the literature. A generic equation has been used to model $C_p(\lambda, \beta)$ and based on the modeling turbine characteristics as appeared in the following equation [57]:

Fig. 6 Aerodynamic power
coefficient variation against
λ and β
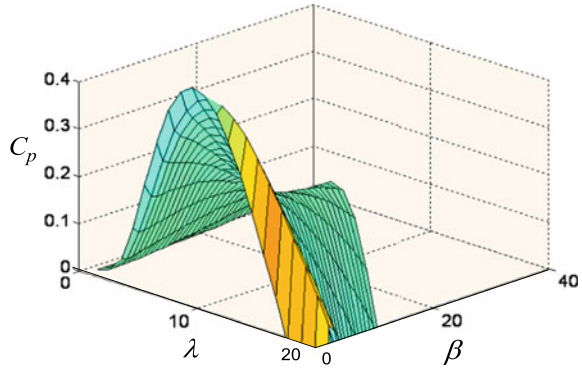
$$C_P(\lambda, \beta) = 0.5176\left(116 * \frac{1}{\lambda_i} - 0.4\beta - 5\right)e^{-\frac{21}{\lambda_i}} + 0.0068\lambda \tag{3}$$

$$\text{With } \frac{1}{\lambda_i} = \frac{1}{\lambda + 0.08\beta} - \frac{0.035}{1 + \beta^3} \tag{4}$$

The C_p-λ characteristics, for different values of the pitch angle β, are illustrated in Fig. 6. The maximum value of C_p is achieved for $\beta = 0°$. The particular value of λ is defined as the optimal value (λ_{opt}). Continuous operation of WT at this point guarantees the maximum available power which can be harvested from the available wind at any speed.

2.1 Electric Generators—Variable Speed Turbines

1. Doubly-Fed Induction Generator (DFIG)

DFIG generators are of the induction type with a coiled rotor and use brushes to feed the rotor windings. The brushes receive energy through a power converter, which can decouple the operating frequency from the grid from the operating frequency of the turbine rotor. The stator is supplied directly by connecting to the grid. Usually, a circuit element called a "crowbar" is used to protect the converter. It has the function of providing a path for the overcurrent arising from electrical transients in the system when they exceed a certain level of design.

The main advantages of this type of machine are the operation with maximum efficiency, the control of active and reactive power, in addition to using lower capacity converters when compared to the FRC configuration. The main disadvantage is the need for slip rings with brushes, thus requiring constant maintenance [73–75]. A typical composition of this wind turbine configuration is shown in Fig. 7 [76].
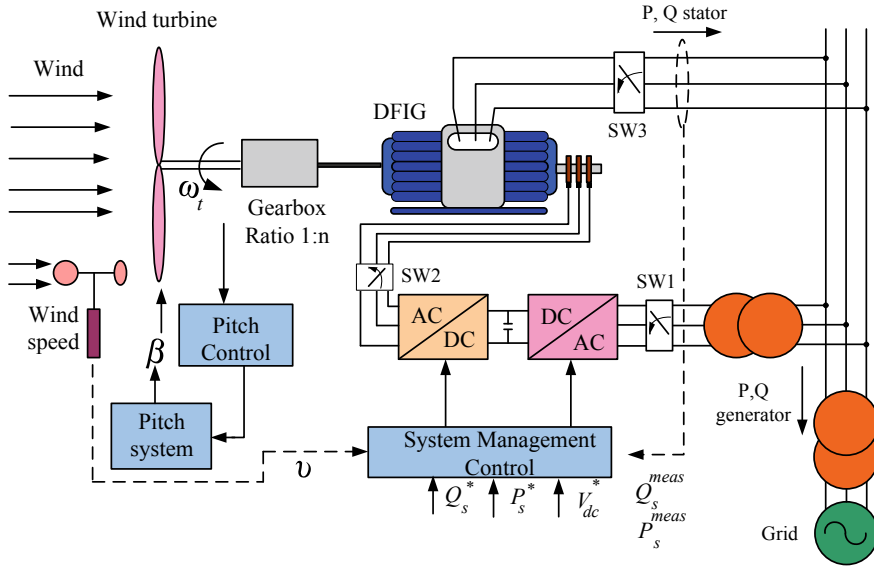
Fig. 7 Typical configuration of DFIG turbines

2. *Fully Rated Converter Wind Turbine (FRC)—Wind Turbine with Full Converter*

This type of configuration is quite versatile, as it may or may not need a speed multiplier and, besides, a range of electric generators can be used: squirrel cage and synchronous generators. As all of the turbine energy flows through converters, the dynamic operation of the generator is isolated from the grid [76].

This isolation is essential for operating at variable speed, as the operating speed of the turbine and, consequently, the operating frequency varies with the wind speed, while the network frequency is stable and varies very little under normal operating conditions. Thus, it is noticed that the power converter is the fundamental device to obtain harmonic integration between variable speed turbines with electrical networks. A typical configuration for this type of system is shown in Fig. 8 [77].

As can be seen in Fig. 8, converters associated with a dc bus can be used interconnecting the turbine with the network output transformer.

A typical operating configuration is to use the grid side converter to keep the voltage level constant, while the converter next to the generator acts to control the generator torque. An alternative way of working is to control the torque of the turbine through the converter next to the grid, while active power is transmitted from the generator to the converters [78].

This system has a disadvantage with the cost of the power converter, since now as all the energy flows through it, it will be necessary to increase the rated power of the converter and thus increase the system.
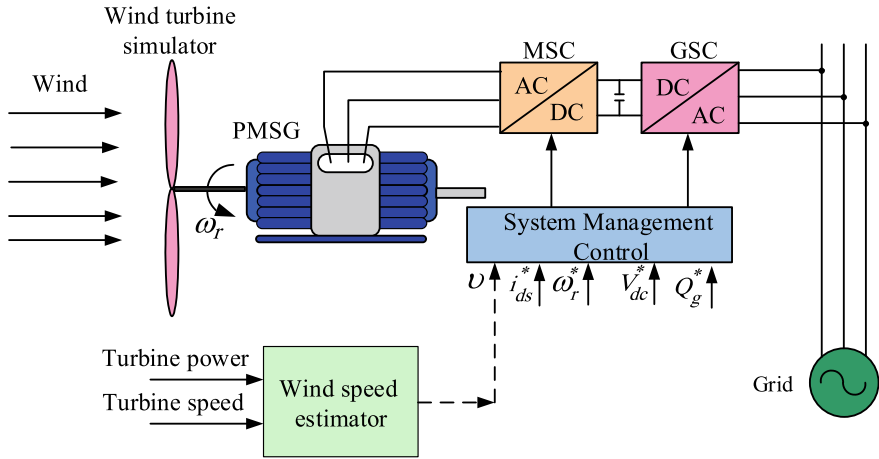
Fig. 8 Typical configuration of FRC turbines [77]

2.2 Wind Generators—Impacts on the Electrical Network

Wind turbines have their peculiarities of operation and integration with the electricity grid when compared to traditional means of power generation (hydroelectric, thermoelectric, and nuclear). Some differences in basic information can be cited [79, 80]:

- The control system for wind turbines is different, with the use of power converters being quite common;
- The driving force that generates energy, the wind, is typically a phenomenon subject to occasional variations and is therefore not controllable;
- The dimensions of the wind generator are much smaller when compared to those of conventional generators and, therefore, a large number of units make up the plant.

Thus, the behavior of the wind turbine in relation to the electrical networks is different, requiring detailed treatment.

1. **Impact on Local Networks**
– **Voltage control**

The influence of wind turbines on local energy networks depends on the type of operation chosen, that is, operation at fixed or variable speed.

For fixed speed, the generator used is the squirrel cage induction generator, which has advantages such as being more economical and easier maintenance compared to other models. However, it is not able to control the grid voltage alone. Thus, the voltage control is done by inserting reactive power through the use of elements external to the system, as in the case of capacitor banks in parallel.

Variable speed turbines are able, in principle, to vary the reactive power exchanged with the grid and, thus, influence the stabilization of the voltage level in the local power grid. This characteristic will depend on the type of converter used specifically for each turbine [81–84].

– **Protection Coordination**

As wind turbines that operate at fixed speed use induction generators, in the event of balanced faults, these only contribute to sub-transitory currents. For unbalanced faults, the contribution of wind turbines to the fault current value is integral.

For turbines operating at variable speed, DFIG generators have at first also contributed to the fault currents in the network. However, as these generators are usually associated with power converters and these converters are quite sensitive to over-currents and have to be quickly disconnected from the grid [85, 86]. Thus, by design, these turbines are quickly disconnected from the network in the event of faults, except for some caveats that are imposed by network codes for the "Ride through Fault" capability.

– **Energy Quality**

Harmonic distortions are more associated with turbines that operate at variable speed, as they use power converters that are great sources of high-frequency harmonic currents. In turbines operating at fixed speed, variations in wind speed are directly transmitted to the generator's output power, thus causing small voltage variations. If the network to which these turbines are connected is "weak", these small voltage variations will be able to generate the phenomenon known as voltage fluctuations and, consequently, flicker [87].

2. **Impact on Global Networks**
– **Grid stability**

For turbines operating at fixed speed using an induction type generator with a squirrel cage rotor, a serious problem that can occur is the rotor's over-speed. The trip occurs due to the occurrence of a fault in the system and the consequent voltage drop of that fault will generate a serious imbalance between the mechanical power generated by the wind and the power generated to the network. After the fault ceases, another problem occurs, which is the absorption of reactants from the generator through the network, contributing to delay in the recovery of voltage in the network. If the system voltage is not restored to nominal values quickly, the turbines tend to accelerate and absorb more reactive power. Thus, it is noticed that fixed speed turbines composed of squirrel cage generators are not able to help maintain the stability of the network, a fact that is essential for delivering quality energy to the consumer.

For variable speed turbines, a risk to the stability of the system is the high sensitivity of the power converters to variations in voltage and current. Thus, if the system has a large presence of this type of turbine (current market trend), and these disconnect for small and medium voltage variations, a large voltage drop will affect the entire

energy system. To avoid this problem, the network codes in general establish the levels of voltage sags to which wind turbines must withstand without disconnecting, thus avoiding large losses of generation power [88, 89].

3 MPPT Control Strategies for the WECS

3.1 Power Signal Feedback (PSF) Control

In PSF control, it is required to have the knowledge of the wind turbine's MP curve, and track this curve through its control mechanisms. The MP curves need to be obtained via simulations or offline experiments on individual WTs or from the datasheet of WT which makes it difficult to implement with accuracy in practical applications. In this method, reference power is generated using an MP data curve or using the mechanical power equation of the WT where wind speed or the rotational speed is used as the input. Figure 9 shows the block diagram of a WECS with the PSF controller for MP extraction. The PSF control block generates the optimal power command P_{opt} which is then applied to the grid side converter control system for MP extraction as appeared in the following equation [72]:

$$P_{opt} = K_{opt} * \omega_r^3 \tag{5}$$

The actual power output, P_t is compared to the optimal power, P_{opt} and any mismatch is used by the fuzzy logic controller to change the modulation index of the grid side converter, PWM-VSC as appeared in Fig. 9. The PWM-VSC is used to interface the WT with the electrical utility and will be controlled through the power angle, δ, and modulation index, m_a to control the active and reactive power output from the WTG [72].
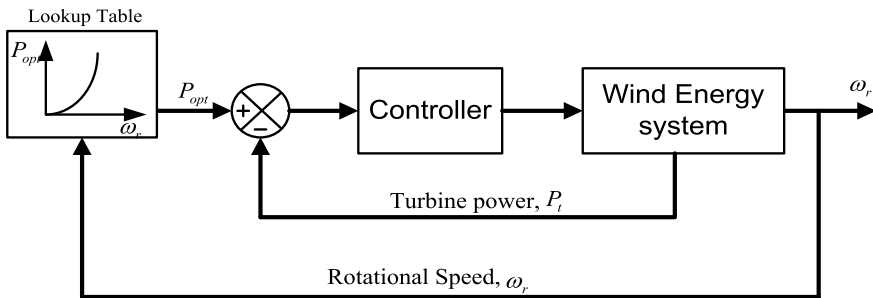
Fig. 9 The block diagram of power signal feedback control [72]

3.2 Optimal Torque Control

The torque controller aims to optimize the efficiency of wind energy capture in a wide range of wind velocities, keeping the power generated by the machine equal to the optimal defined value. It can be observed from the block diagram represented in Fig. 10, that the idea of this method is to adjust the PMSG torque according to the optimal reference torque of the WT at a given wind speed. A typical WT characteristic with the optimal torque-speed curve plotted to intersect the $C_{P\text{-max}}$ points for each wind speed is illustrated in Fig. 11. The curve T_{opt} defines the optimal torque of the device (i.e. maximum energy capture), and the control objective is to keep the turbine on this curve as the wind speed varies. For any wind speed, the MPPT device imposes a torque reference able to extract the MP. The curve T_{opt} is defined by the following equation [70]:

$$T_{opt} = K_{opt} * \omega_{opt}^2 \tag{6}$$
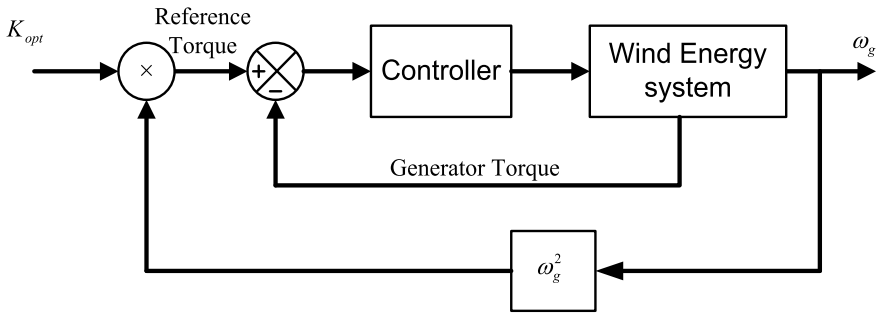
Fig. 10 The block diagram of optimal torque control MPPT method
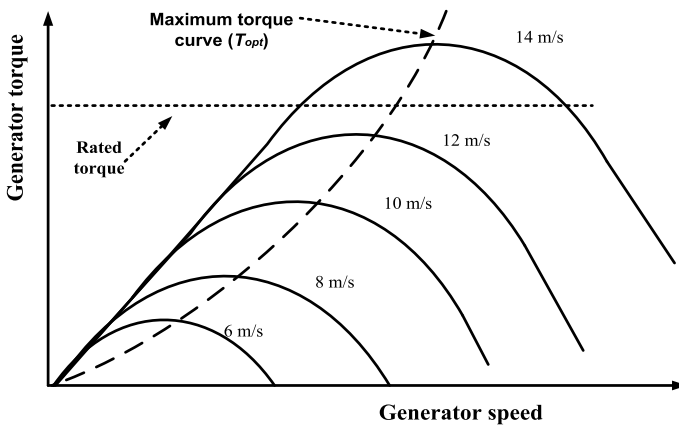
Fig. 11 Wind turbine characteristic for MP extraction [70]

where, $K_{opt} = 0.5 * \rho A * \left(\frac{r_m}{\lambda_{opt}}\right)^3 * C_{P-\max}$.

4 Decoupled Control of the Active and Reactive Power

In this study, a simple ac-dc-ac power conversion system and proposed a modular control strategy for grid-connected wind power generation systems have been implemented [65]. Grid side inverter maintains the dc-link voltage constant and the power factor of the line side can be adjusted. Input current reference of DC/DC boost converter is decided for the MPPT of the turbine without any information on wind or generator speed. As the proposed control algorithm does not require any speed sensor for wind or generator speed, construction and installation are simple, cheap, and reliable. The main circuit and control block diagrams have appeared in Fig. 12. For a wide range of variable speed operations, a dc-dc boost converter is utilized between a 3-phase diode rectifier and PWM-VSC. The input dc current is regulated to follow the optimized current reference for MPP operation of the turbine system. Grid PWM-VSC supply currents into the utility line by regulating the dc-link voltage. The active power is controlled by q-axis current through regulating the dc-link voltage whereas the reactive power can be controlled by d-axis current via adjusting the power factor of the grid side converter. The phase angle of utility voltage is detected using Phase Locked Loop, *PLL*, in d-q synchronous reference frame [65].
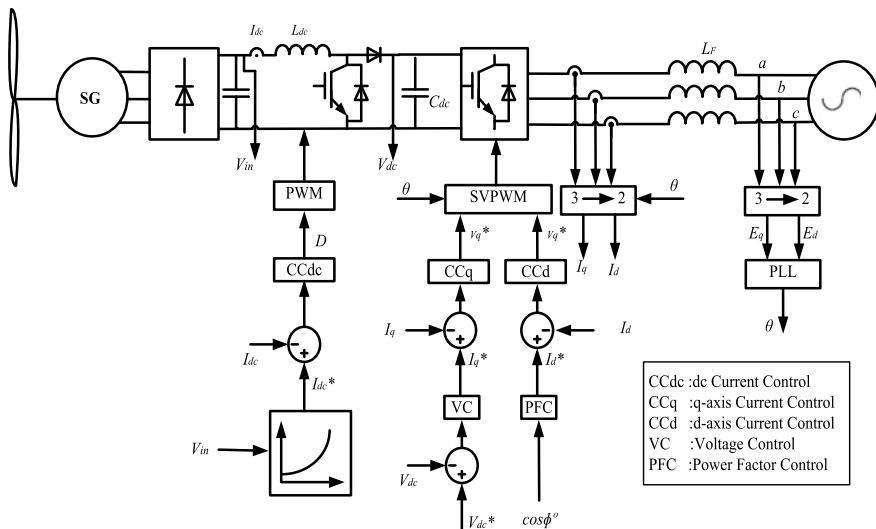
Fig. 12 Block diagram of system control [65]
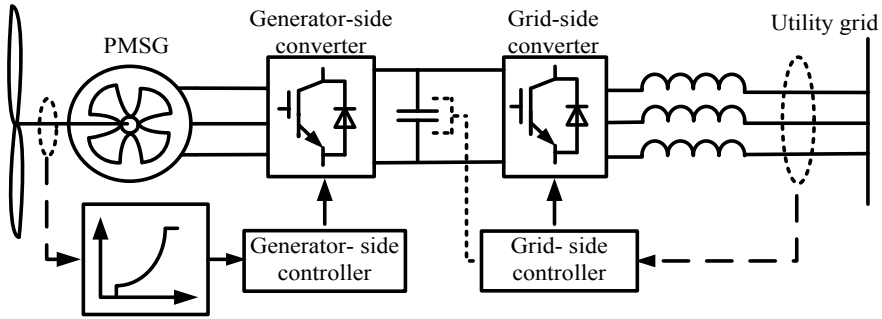
Fig. 13 Schematic diagram of the overall system [52, 55, 56]

4.1 Co-Simulation (PSIM/MATLAB) Program for Interconnecting Wind Energy System with Electric Utility

In this study, the WECS is designed as PMSG connected to the grid via a back-to-back PWM-VSC as appeared in Fig. 13. MPPT control algorithm has been introduced using FLC to regulate the rotational speed to force the PMSG to work around its MPP in speeds below rated speeds and to produce the rated power in wind speed higher than the rated wind speed of the WT. An indirect vector-controlled PMSG system has been used for this purpose. The input to FLC is two real-time measurements which are the change of output power and rotational speed between two consequent iterations (ΔP, and $\Delta \omega_m$). The output from FLC is the required change in the rotational speed $\Delta \omega_{m\text{-}new}*$. The detailed logic behind the newly proposed technique is explained in detail in the following sections. Two effective computer simulation software packages (PSIM and SIMULINK) have been used to carry out the simulation effectively where PSIM contains the power circuit of the WECS and MATLAB/SIMULINK contains the control circuit of the system. The idea behind using these two different software packages is the effective tools provided with PSIM for power circuit and the effective tools in SIMULINK for control circuit and FLC.

4.2 Wind Energy Conversion System Description

Figure 14 shows a co-simulation (PSIM/SIMULINK) program for interconnecting WECS to electric utility. The PSIM program contains the power circuit of the WECS and MATLAB/SIMULINK program contains the control of this system. The interconnection between PSIM and MATLAB/SIMULINK has been done via the SimCoupler block. The basic topology of the power circuit which has PMSG-driven WT connected to the utility grid through the ac-dc-ac conversion system has appeared in Fig. 13.
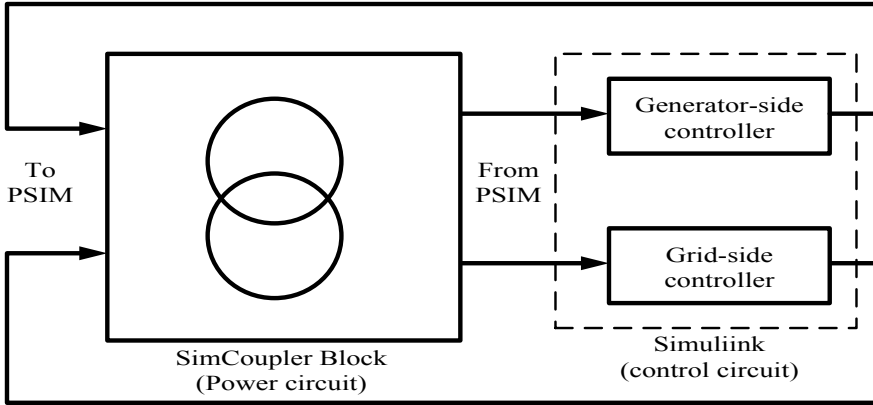
Fig. 14 Co-simulation block of wind energy system interfaced with the electric utility

The PMSG is connected to the grid through back-to-back bidirectional PWM voltage source converters VSC. The generator side converter is used as a rectifier, while the grid side converter is used as an inverter. The generator side converter is connected to the grid side converter through dc-link capacitor. The control of the overall system has been done through the generator side converter and the grid side converter. MPPT algorithm has been achieved by controlling the generator side converter using FLC. The grid side converter controller maintains the dc-link voltage at the desired value by exporting active power to the grid and it controls the reactive power exchange with the grid.

1. *PMSG Model*

The voltage equation of the three-phase PMSG type is defined as follows [73].

$$
\begin{bmatrix} v_{as} \\ v_{bs} \\ v_{cs} \end{bmatrix} = \begin{bmatrix} R_s + \frac{d}{dt}(l_{as} + M) & \frac{-1}{2}\frac{d}{dt}M & \frac{-1}{2}\frac{d}{dt}M \\ \frac{-1}{2}\frac{d}{dt}M & R_s + \frac{d}{dt}(l_{bs} + M) & \frac{-1}{2}\frac{d}{dt}M \\ \frac{-1}{2}\frac{d}{dt}M & \frac{-1}{2}\frac{d}{dt}M & R_s + \frac{d}{dt}(l_{cs} + M) \end{bmatrix} \begin{bmatrix} i_{as} \\ i_{bs} \\ i_{cs} \end{bmatrix} + \begin{bmatrix} e_{as} \\ e_{bs} \\ e_{cs} \end{bmatrix}
\tag{7}
$$

where v_{as}, v_{bs}, and v_{cs} are stator a, b, and c phase voltages, and i_{as}, i_{bs}, and i_{cs} are stator a, b, and c phase currents. The electromotive force induced in the stator windings of phases a, b, and c are e_{as}, e_{bs}, and e_{cs}, R_s is the stator winding resistance, l_s is the leakage inductance of the stator winding, and M is the mutual inductance between the stator windings. In a balanced 3-phase circuit, the sum of each phase current becomes 0, and when $L_s = l_s + (3/2)M$ (equivalent inductance (L_s)), the voltage equation is simplified as follows:

$$
\begin{bmatrix} v_{as} \\ v_{bs} \\ v_{cs} \end{bmatrix} = \begin{bmatrix} R_s + \frac{d}{dt}L_s & 0 & 0 \\ 0 & R_s + \frac{d}{dt}L_s & 0 \\ 0 & 0 & R_s + \frac{d}{dt}L_s \end{bmatrix} \begin{bmatrix} i_{as} \\ i_{bs} \\ i_{cs} \end{bmatrix} + \begin{bmatrix} e_{as} \\ e_{bs} \\ e_{cs} \end{bmatrix} \tag{8}
$$

$$
v_{as} = R_s i_{as} + L_s \frac{d}{dt} i_{as} + e_{as} \tag{9}
$$

$$
v_{bs} = R_s i_{bs} + L_s \frac{d}{dt} i_{bs} + e_{bs} \tag{10}
$$

$$
v_{cs} = R_s i_{cs} + L_s \frac{d}{dt} i_{cs} + e_{cs} \tag{11}
$$

Equations (9)–(11) can be integrated into a vector form as follows:

$$
v_{abcs} = R_s I_{abcs} + L_s \frac{d I_{abcs}}{dt} + E_{abcs} \tag{12}
$$

If the number of fluxes crossing the stator winding by the rotor of the PMSG is called *epsa*, *epsb*, and *epsc*, and the maximum value of the flux is *epsf*, the magnitude of the flux crossing the stator winding is as follows:

$$
\Psi_a = \Psi_f \cos\theta
$$

$$
\Psi_b = \Psi_f \cos\left(\theta - \frac{2}{3}\pi\right)
$$

$$
\Psi_c = \Psi_f \cos\left(\theta + \frac{2}{3}\pi\right) \tag{13}
$$

At this time, the synchronous phase angle θ was calculated as the rotational speed ω_r. If $\theta = \int \omega_r dt$, the electromotive force induced in the three-phase stator winding is defined as follows:

$$
e_{as} = -\omega_r \Psi_f \sin\theta
$$

$$
e_{bs} = -\omega_r \Psi_f \sin\left(\theta - \frac{2}{3}\pi\right)
$$

$$
e_{cs} = -\omega_r \Psi_f \sin\left(\theta + \frac{2}{3}\pi\right) \tag{14}
$$

To convert a 3-phase state equation to a *d-q* stationary reference frame ($\omega = 0$), multiply the following transformation matrix:

$$T(0) = \begin{bmatrix} 1 & 0 & 0 \\ 0 & \frac{1}{\sqrt{3}} & \frac{-1}{\sqrt{3}} \end{bmatrix} \tag{15}$$

Multiplying Eq. (12) by Eq. (15):

$$T(0)v_{abcs} = R_s T(0) I_{abcs} + L_s \frac{dI_{abcs}}{dt} T(0) + T(0) E_{abcs}$$

$$V^S_{dqs} = R_s I^S_{dqs} + L_s \frac{d}{dt} I^S_{dqs} + E^S_{dqs} \tag{16}$$

The electromotive force induced to the stator is obtained as follows by substituting Eq. (13) into Eq. (16) as follows:

$$E_{abcs} = \begin{bmatrix} -\omega_r \Psi_f \sin\theta \\ \omega_r \Psi_f \cos\theta \end{bmatrix} \tag{17}$$

The flux linkage of the stationary system is as follows:

$$\begin{bmatrix} \Psi^s_{ds} \\ \Psi^s_{qs} \end{bmatrix} = T(0) \begin{bmatrix} \Psi_f \cos\theta \\ \Psi_f \cos(\theta - \frac{2}{3}\pi) \\ \Psi_f \cos(\theta + \frac{2}{3}\pi) \end{bmatrix} = \begin{bmatrix} \Psi_f \cos\theta \\ \Psi_f \sin\theta \end{bmatrix} \tag{18}$$

To perform the control of a rotating device, the state equation of the stationary coordinate system must be converted into a synchronous coordinate system:

$$V^S_{dqs} = R_s I^e_{dqs} + L_s \frac{d}{dt} I^e_{dqs} + L_s \begin{bmatrix} 0 & -\omega_r \\ -\omega_r & 0 \end{bmatrix} + E^e_{dqs} \tag{19}$$

If the 3-phase state equation is changed to the synchronous coordinate system d-q, it is as shown in Eq. (19), and rearranged as follows:

$$\begin{bmatrix} v^e_{ds} \\ v^e_{qs} \end{bmatrix} = \begin{bmatrix} R_s + \frac{dL_s}{dt} & -\omega_r L_s \\ -\omega_r L_s & R_s + \frac{dL_s}{dt} \end{bmatrix} \begin{bmatrix} i^e_{ds} \\ i^e_{qs} \end{bmatrix} + \begin{bmatrix} e^e_{ds} \\ e^e_{qs} \end{bmatrix} \tag{20}$$

The stator induced EMF can be expressed as follows:

$$\begin{bmatrix} e^e_{ds} \\ e^e_{qs} \end{bmatrix} = \begin{bmatrix} 0 \\ \omega_r \Psi_f \end{bmatrix} \tag{21}$$

Finally, the PMSG's synchronous coordinate system d-q voltage equation can be obtained.

$$\begin{bmatrix} v_{ds}^e \\ v_{qs}^e \end{bmatrix} = \begin{bmatrix} R_s + \frac{dL_s}{dt} & -\omega_r L_s \\ -\omega_r L_s & R_s + \frac{dL_s}{dt} \end{bmatrix} \begin{bmatrix} i_{ds}^e \\ i_{qs}^e \end{bmatrix} + \begin{bmatrix} 0 \\ \omega_r \Psi_f \end{bmatrix} \tag{22}$$

Since the rotor of the PMSG has no energy input and output, it can be regarded as electromagnetic torque, which can be expressed as follows:

$$T_e = \frac{3}{2} P \psi_F i_{qs} \tag{23}$$

where, P is the number of pole pairs.

5 Control of the Generator Side Converter (PMSG)

The generator side controller controls the rotational speed to produce the maximum output power via controlling the electromagnetic torque according to Eq. (10), where the indirect vector control is used. The proposed control logic of the generator side converter appears in Fig. 15. The speed loop will generate the q-axis current component to control the generator torque and speed at different wind speed via estimating the reference value of i_α, i_β as appeared in Fig. 15. The torque control can be achieved through the control of the i_{sq} current. Figure 16 shows the stator and rotor current space phasors and the excitation flux of the PMSG. The quadrature stator current i_{sq} can be controlled through the rotor reference frame (α, β axis) as appeared in Fig. 16. So, the reference value of i_α, i_β can be estimated easily from the amplitude of i_{sq*} and the rotor angle, θ_r. Initially, to find the rotor angle, θ_r, the relationship between the electrical angular speed, ω_r, and the rotor mechanical speed (rad/s), ω_m may be expressed as:
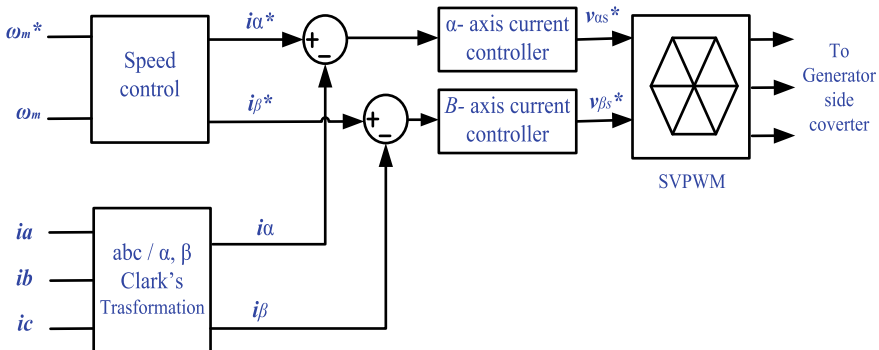
Fig. 15 Control block diagram of PMSG
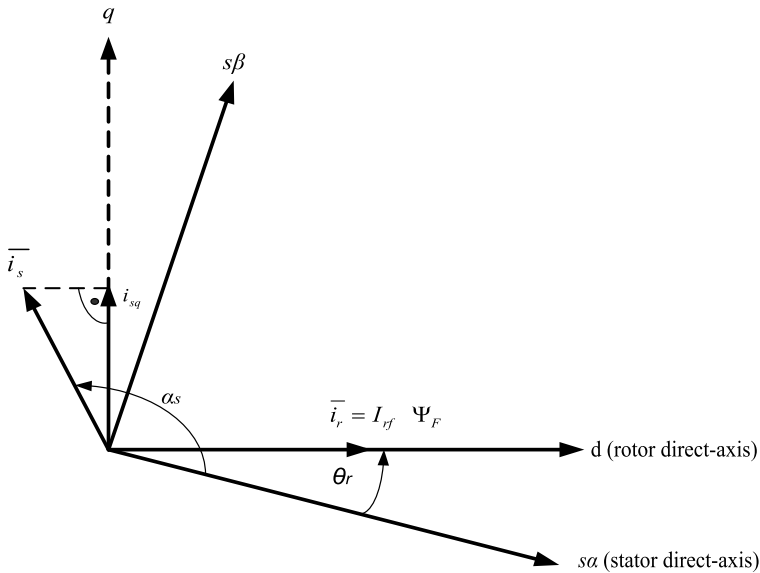
Fig. 16 The stator and rotor current space phasors and the excitation flux of the PMSG

$$\omega_r = \frac{P}{2}\omega_m \tag{24}$$

So, the rotor angle, θ_r, can be estimated by integrating the electrical angular speed, ω_r. The input to the speed control is the actual and reference rotor mechanical speed (rad/s) and the output is the (α, β) reference current components. The actual values of the (α, β) current components are estimated using Clark's transformation to the three-phase current of PMSG. The FLC can be used to find the reference speed along which tracks the MPP.

5.1 Fuzzy Logic Controller for MPPT

At a certain wind speed, the power is maximum at a certain ω called optimum rotational speed, ω_{opt}. This speed corresponds to the optimum tip speed ratio, λ_{opt} [71]. So, to extract MP at variable wind speed, the turbine should always operate at λ_{opt}. This occurs by controlling the rotational speed of the turbine. Controlling the turbine to operate at optimum rotational speed can be done using the fuzzy logic controller. Each WT has one value of λ_{opt} at variable speed but ω_{opt} changes from certain wind speed to another. From Eq. (6), the relation between ω_{opt} and wind speed, u, for constant R and λ_{opt} can be deduced as appeared in (25):

$$\omega_{opt} = \frac{\lambda_{opt}}{R}u \qquad (25)$$

From Eq. (25), the relation between the optimum rotational speed and wind speed is linear. At a certain wind speed, there is an optimum rotational speed which is different at another wind speed. The fuzzy logic control is used to search (observation and perturbation) the rotational speed reference which tracks the MPP at variable wind speeds. The fuzzy logic controller block diagram appears in Fig. 17. Two real-time measurements are used as input to fuzzy (ΔP, and $\Delta\omega_m{}^*$) and the output is ($\Delta\omega_{m-new}{}^*$). Membership functions appear in Fig. 18. Triangular symmetrical membership functions are suitable for the input and output, which give more sensitivity especially as variables approach zero value. The width of variation can
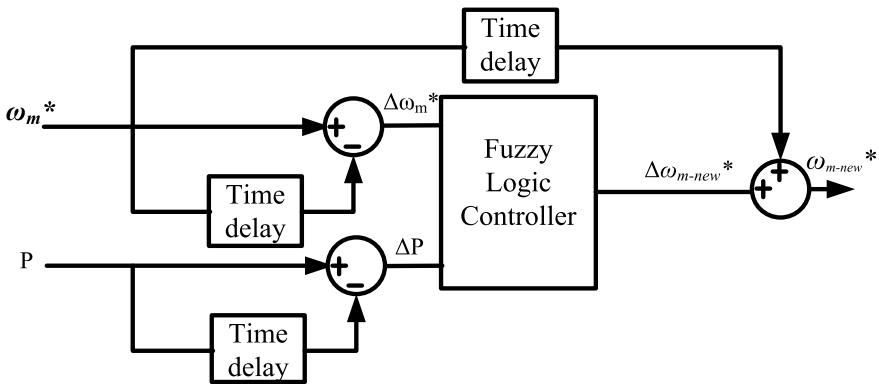
Fig. 17 Input and output of fuzzy controller
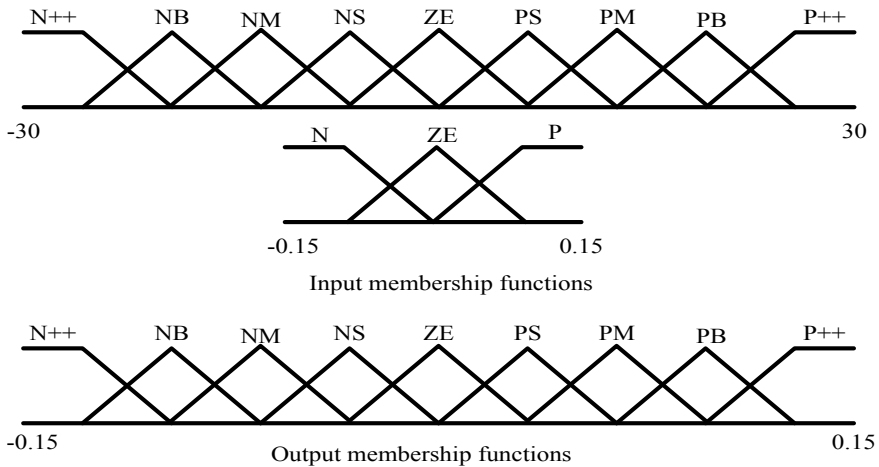
Fig. 18 Membership functions of the fuzzy logic controller

Table 1 Rules of fuzzy logic controller

$\frac{\Delta P}{\Delta \omega_m}$	N++	NB	NM	NS	ZE	PS	PM	PB	P++
N	P++	PB	PM	PS	ZE	NS	NM	NB	N++
ZE	NB	NM	NS	NS	ZE	PS	PM	PM	PB
P	N++	NB	NM	NS	ZE	PM	PM	PB	PB

be adjusted according to the system parameter. The input signals are first fuzzified and expressed in fuzzy set notation using linguistic labels which are characterized by membership functions before it is processed by the FLC. Using a set of rules and a fuzzy set theory, the output of the FLC is obtained. This output, expressed as a fuzzy set using linguistic labels characterized by membership functions, is defuzzified and then produces the controller output. The fuzzy logic controller doesn't require any detailed mathematical model of the system and its operation is governed simply by a set of rules. The principle of the fuzzy logic controller is to perturb the reference speed ω_m* and to observe the corresponding change of power, ΔP. If the output power increases with the last increment, the searching process continues in the same direction. On the other hand, if the speed increment reduces the output power, the direction of the searching is reversed. The fuzzy logic controller is efficient to track the MPP, especially in case of frequently changing wind conditions.

Figure 18 shows the input and output membership functions and Table 1 lists the control rule for the input and output variable. The next fuzzy levels are chosen for controlling the inputs and output of the fuzzy logic controller. The variation step of the power and the reference speed may vary depending on the system. In Fig. 18, the variation step in the speed reference is from −0.15 to 0.15 rad/s for power variation ranging over from −30 to 30 W. The membership definitions are given as follows: N (negative), N++ (very big negative), NB (negative big), NM (negative medium), NS (negative small), ZE (zero), P (positive), PS (positive small), PM (positive medium), PB (positive big), and P++ (very big positive).

5.2 Control of the Grid Side Converter

The power flow of the grid side converter is controlled in order to maintain the dc-link voltage at reference value, 600 V. Since increasing the output power than the input power to dc-link capacitor causes a decrease of the dc-link voltage and vice versa, the output power will be regulated to keep dc-link voltage approximately constant. To maintain the dc-link voltage constant and to ensure the reactive power flowing into the grid, the grid side converter currents are controlled using the d-q vector control approach. The dc-link voltage is controlled to the desired value by using a PI-controller and the change in the dc-link voltage represents a change in the q-axis (i_{qs}) current component. Figure 19 shows a control block diagram of the grid side converter. The active power can be defined as appeared in the following equation:
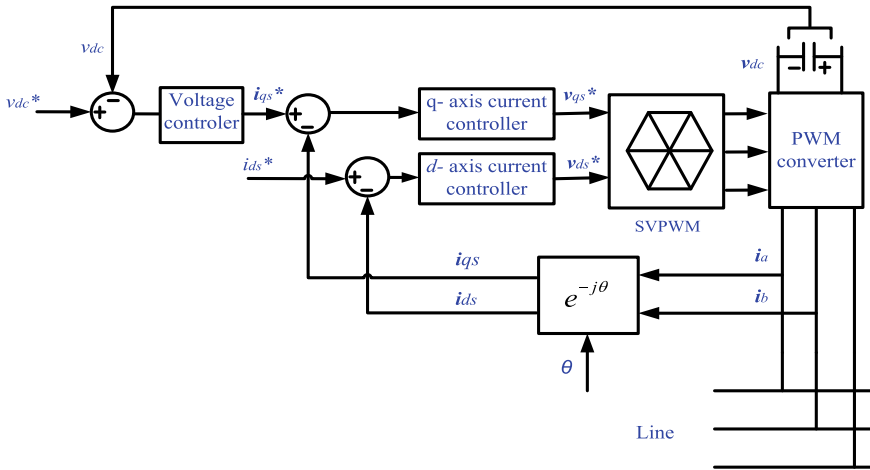
Fig. 19 Control block diagram of grid side converter [55, 56]

$$P_s = \frac{3}{2}\left(v_{ds}i_{ds} + v_{qs}i_{qs}\right) \tag{26}$$

The reactive power can be defined as:

$$Q_s = \frac{3}{2}\left(v_{qs}i_{ds} - v_{ds}i_{qs}\right) \tag{27}$$

By aligning the q-axis of the reference frame along with the grid voltage position $v_{ds} = 0$ and $v_{qs} = $ constant because the grid voltage is assumed to be constant. Then the active and reactive power can be obtained from the following equations:

$$P_s = \frac{3}{2}v_{qs}i_{qs} \tag{28}$$

$$Q_s = \frac{3}{2}v_{qs}i_{ds} \tag{29}$$

6 Simulation Results and Discussion

A co-simulation (PSIM/SIMULINK) program has been used where PSIM contains the power circuit of the WECS and MATLAB/SIMULINK has the whole control system as described before. The model of WECS in PSIM contains the WT connected to the utility grid through a back-to-back bidirectional PWM converter. The control of the whole system in SIMULINK contains the generator side controller and the

grid side controller. The generator can be directly controlled by the generator side controller to track the MP available from the WT. The wind speed is variable and changes from 7 to 13 m/s as input to WT. To extract MP at variable wind speed, the turbine should always operate at λ_{opt}. This occurs by controlling the rotational speed of the WT. So, it always operates at the optimum rotational speed. ω_{opt} changes from certain wind speed to another. The fuzzy logic controller is used to search the optimum rotational speed which tracks the MPP at variable wind speeds. Figure 20a shows the variation of the wind speed which varies randomly from 7 to13 m/s. On the other hand, Fig. 20b shows the variation of the actual and reference rotational speed as a result of the wind speed variation. At a certain wind speed, the actual and reference rotational speed has been estimated and this agreement with the power characteristic of the WT appeared later in Fig. 14. i.e. the WT always operates at the optimum rotational speed which is found using FLC; hence, the power extraction from wind is maximum at variable wind speed. It is seen that according to the wind speed variation the generator speed varies and that its output power is produced corresponding to the wind speed variation. The fuzzy logic controller works well and it gives a good tracking performance for the MPP. The fuzzy logic controller makes WT always operates at the optimum rotational speed. On the other hand, the grid side controller maintains the dc-link voltage at the desired value, 600v, as appeared in Fig. 20c. The dc-link voltage is regulated by exporting active power to the grid as appeared in Fig. 20d. The reactive power transmitted to the grid appears in Fig. 20e.

7 Conclusion

Variable speed operation and direct drive wind turbines (WTs) have been considered as the modern aspects of wind energy conversion systems (WECS). In this chapter, a fuzzy logic controller (FLC)-based MPPT strategy for (WECS) is proposed. The generator side controller has been used to track the maximum power generated from WTs through controlling the rotational speed of the WT using FLC. The performance of the proposed MPPT strategy is analyzed mathematically and verified by simulation using MATLAB/PSIM/Simulink software. The PMSG has been controlled in an indirect vector field-oriented control technique and its speed reference has been obtained from FLC. The simulation outcomes have been conducted to approve the performance of the proposed MPPT strategy, and all results have confirmed the adequacy of the proposed MPPT strategy.
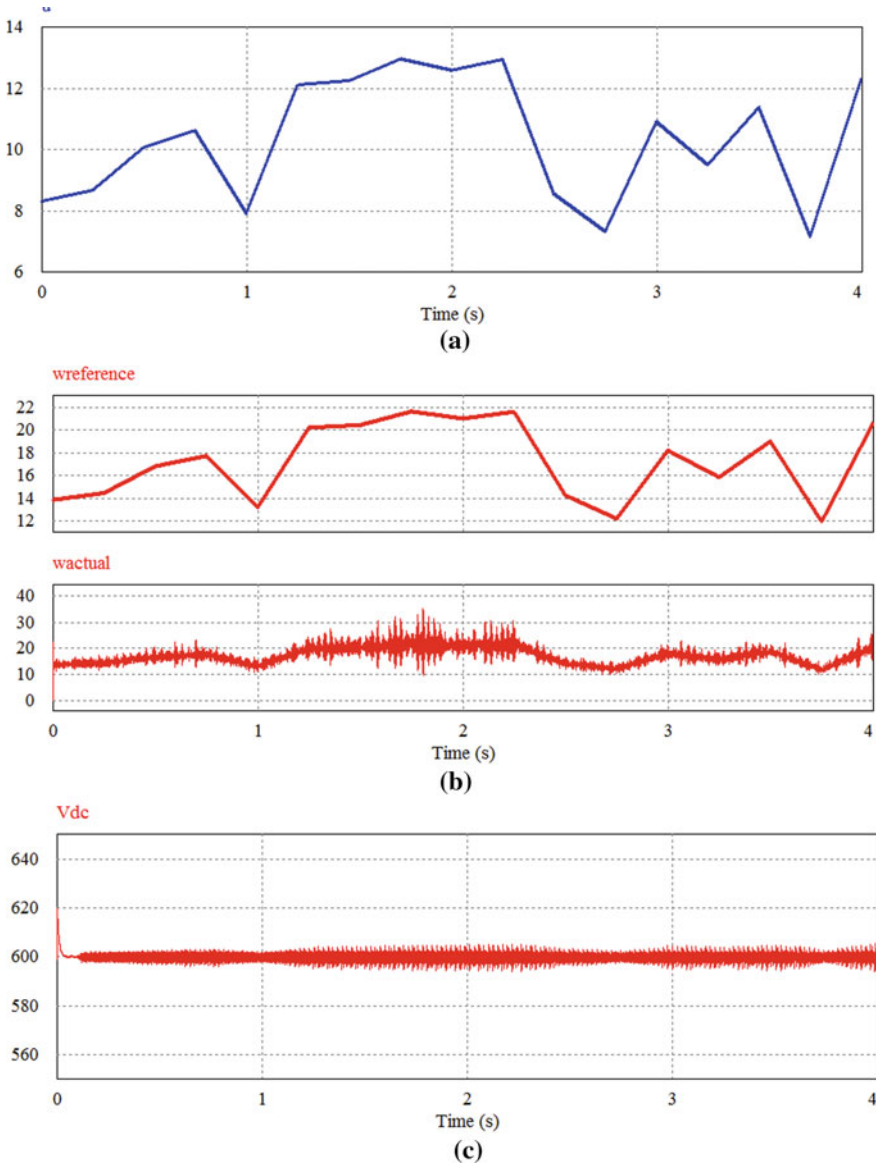
Fig. 20 Different simulation waveforms: **a** wind speed variation (7–13) m/s. **b** actual and reference rotational speed (rad/s). **c** dc-link voltage (V). **d** Active power (W). **e** Reactive power (Var)

(d)

(e)
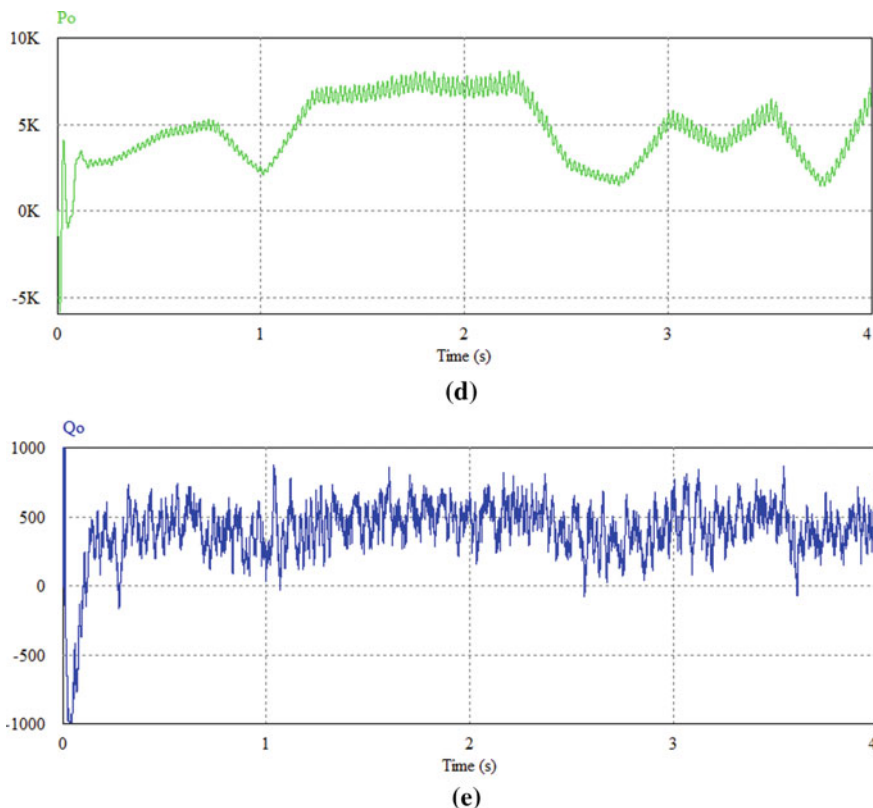
Fig. 20 (continued)

References

1. Ahmed MA, Eltamaly AM, Alotaibi MA, Alolah AI, Kim Y-C (2020) Wireless network architecture for cyber physical wind energy system. IEEE Access 8:40180–40197
2. Eltamaly AM, Addoweesh KE, Bawa U, Mohamed MA (2014) Economic modeling of hybrid renewable energy system: a case study in Saudi Arabia. Arab J Sci Eng 39(5):3827–3839
3. Eltamaly AM, Al-Saud M, Sayed K, Abo-Khalil AG (2020) Sensorless active and reactive control for DFIG wind turbines using opposition-based learning technique. Sustainability 12(9):3583
4. Eltamaly AM, Mohamed MA (2014) A novel design and optimization software for autonomous PV/wind/battery hybrid power systems. Math Probl Eng
5. Mohamed MA, Jin T, Su W (2020) An effective stochastic framework for smart coordinated operation of wind park and energy storage unit. Appl Energy 272:115228
6. Al-Saud MS, Eltamaly AM, Al-Ahmari A (2017) Multi-rotor vertical axis wind turbine. U.S. patent 9,752,556, 5 Sept 2017
7. Abo-Khalil AG, Ali Alghamdi IT, Eltamaly AM (2019) Current controller design for DFIG-based wind turbines using state feedback control. IET Renew Power Gener 13(11):1938–1948

8. Eltamaly AM, Addoweesh KE, Bawah U, Mohamed MA (2013) New software for hybrid renewable energy assessment for ten locations in Saudi Arabia. J Renew Sustain Energy 5(3):033126

9. Eltamaly AM (2014) Pairing between sites and wind turbines for Saudi Arabia Sites. Arab J Sci Eng 39(8):6225–6233

10. Jin T, Guo J, Mohamed MA, Wang M (2019) A novel model predictive control via optimized vector selection method for common-mode voltage reduction of three-phase inverters. IEEE Access 7:95351–95363

11. Eltamaly AM (2013) Design and implementation of wind energy system in Saudi Arabia. Renew Energy 60:42–52

12. Eltamaly AM (2013) Design and simulation of wind energy system in Saudi Arabia. In: 2013 4th international conference on intelligent systems, modelling and simulation. IEEE, pp 376–383

13. Eltamaly AM, Alolah AI, Farh HM, Arman H (2013) Maximum power extraction from utility-interfaced wind turbines. New Dev Renew Energy 159–192

14. Eltamaly AM, Al-Saud MS (2018) Nested multi-objective PSO for optimal allocation and sizing of renewable energy distributed generation. J Renew Sustain Energy 10(3):035302

15. Aziz MS, Mufti GM, Ahmad S (2017) Wind-hybrid power generation systems using renewable energy sources-a review. Int J Renew Energy Res (IJRER) 7(1):111–127

16. Mohamed MA, Eltamaly AM, Alolah AI, Hatata AY (2019) A novel framework-based cuckoo search algorithm for sizing and optimization of grid-independent hybrid renewable energy systems. Int J Green Energy 16(1):86–100

17. Savino MM, Manzini R, Selva VD, Accorsi R (2017) A new model for environmental and economic evaluation of renewable energy systems: the case of wind turbines. Appl Energy 189:739–752

18. Eltamaly AM, Mohamed MA (2018) Optimal sizing and designing of hybrid renewable energy systems in smart grid applications. Advances in renewable energies and power technologies. Elsevier, pp 231–313

19. Olatayo KI, Wichers JH, Stoker PW (2018) Energy and economic performance of small wind energy systems under different climatic conditions of South Africa. Renew Sustain Energy Rev 98:376–392

20. Mohamed MA, Eltamaly AM, Farh HM, Alolah AI (2015) Energy management and renewable energy integration in smart grid system. In: 2015 IEEE international conference on smart energy grid engineering (SEGE). IEEE, pp 1–6

21. Mohamed MA, Eltamaly AM, Alolah AI (2016) PSO-based smart grid application for sizing and optimization of hybrid renewable energy systems. PLoS ONE 11(8):e0159702

22. Mabrouk IB, Hami AE, Walha L, Zghal B, Haddar M (2017) Dynamic vibrations in wind energy systems: application to vertical axis wind turbine. Mech Syst Signal Process 85:396–414

23. Gandomkar A, Parastar A, Seok J-K (2016) High-power multilevel step-up DC/DC converter for offshore wind energy systems. IEEE Trans Ind Electron 63(12):7574–7585

24. Eltamaly AM, Mohamed MA, Alolah AI (2016) A novel smart grid theory for optimal sizing of hybrid renewable energy systems. Sol Energy 124:26–38

25. Liu S-Y, Ho Y-F (2016) Wind energy applications for Taiwan buildings: what are the challenges and strategies for small wind energy systems exploitation? Renew Sustain Energy Rev 59:39–55

26. Eltamaly AM, Mohamed MA (2016) A novel software for design and optimization of hybrid power systems. J Braz Soc Mech Sci Eng 38(4):1299–1315

27. Salari ME, Coleman J, Toal D (2019) Analysis of direct interconnection technique for offshore airborne wind energy systems under normal and fault conditions. Renew Energy 131:284–296

28. Eltamaly AM, El-Tamaly H, Enjeti P (2001) New modular wind energy conversion system. In: The 8th international middle-east power systems conference MEPCON' 2001, University of Helwan, Cairo, Egypt, 29–31 Dec 2001

29. Kececioglu OF, Acikgoz H, Yildiz C, Gani A, Sekkeli M (2017) Power quality improvement using hybrid passive filter configuration for wind energy systems. J Electr Eng Technol 12(1):207–216

30. Mohamed MA, Eltamaly AM (2018) A novel smart grid application for optimal sizing of hybrid renewable energy systems. Modeling and simulation of smart grid integrated with hybrid renewable energy systems. Springer, Cham, pp 39–51
31. Manwell JF, McGowan JG, Rogers AL (2010) Wind energy explained: theory, design and application. Wiley
32. Raju AB, Fernandes BG, Chatterjee K (2004) A UPF power conditioner with maximum power point tracker for grid connected variable speed wind energy conversion system. In: Proceedings. 2004 first international conference on power electronics systems and applications. IEEE, pp 107–112
33. Mohamed MA, Eltamaly AM (2018) Modeling of hybrid renewable energy system. Modeling and simulation of smart grid integrated with hybrid renewable energy systems. Springer, Cham, pp 11–21
34. Mohamed MA, Eltamaly AM, Alolah AI (2015) Sizing and techno-economic analysis of stand-alone hybrid photovoltaic/wind/diesel/battery power generation systems. J Renew Sustain Energy 7(6):063128
35. Bottiglione F, Mantriota G, Valle M (2018) Power-split hydrostatic transmissions for wind energy systems. Energies 11(12):3369
36. Mohamed MA, Eltamaly AM (2018) A PSO-based smart grid application for optimum sizing of hybrid renewable energy systems. Modeling and simulation of smart grid integrated with hybrid renewable energy systems. Springer, Cham, pp 53–60
37. El-Tamaly AM, Enjeti PN, El-Tamaly HH (2000) An improved approach to reduce harmonics in the utility interface of wind, photovoltaic and fuel cell power systems. In APEC 2000, fifteenth annual IEEE applied power electronics conference and exposition (Cat. No. 00CH37058), vol 2. IEEE, pp 1059–1065
38. Abo-Khalil AG, Lee DC (22008) Maximum power point tracking based on sensorless wind speed using support vector regression. IEEE Trans Ind Electron 55(3)
39. Mohamed MA, Eltamaly AM (2018) Sizing and techno-economic analysis of stand-alone hybrid photovoltaic/wind/diesel/battery energy systems. Modeling and simulation of smart grid integrated with hybrid renewable energy systems. Springer, Cham, pp 23–38
40. Bafandeh A, Vermillion C (2016) Real-time altitude optimization of airborne wind energy systems using Lyapunov-based switched extremum seeking control. In: 2016 American control conference (ACC). IEEE, pp 4990–4995
41. El-Tamaly AM, El-Tamaly HH, Cengelci E, Enjeti PN, Muljadi E (1999) Low cost PWM converter for utility interface of variable speed wind turbine generators. In: Fourteenth annual applied power electronics conference and exposition, APEC'99, conference proceedings (Cat. No. 99CH36285), vol 2. IEEE, pp 889–895
42. Eltamaly AM, Al-Saud MS, Abo-Khalil AG (2020) Dynamic control of a DFIG wind power generation system to mitigate unbalanced grid voltage. IEEE Access 8:39091–39103
43. Li Y, Feng Bo, Li G, Qi J, Zhao D, Yunfei Mu (2018) Optimal distributed generation planning in active distribution networks considering integration of energy storage. Appl Energy 210:1073–1081
44. Eltamaly AM (2002) New formula to determine the minimum capacitance required for self-excited induction generator. In: 2002 IEEE 33rd annual IEEE power electronics specialists conference. Proceedings (Cat. No. 02CH37289), vol 1. IEEE, pp. 106–110
45. Koutsoukis NC, Siagkas DO, Georgilakis PS, Hatziargyriou ND (2016) Online reconfiguration of active distribution networks for maximum integration of distributed generation. IEEE Trans Autom Sci Eng 14(2):437–448
46. Hamouda RM, Eltamaly AM, Alolah AI (2008) Transient performance of an isolated induction generator under different loading conditions. In: 2008 Australasian Universities power engineering conference. IEEE, pp 1–5
47. Novakovic B, Nasiri A (2017) Modular multilevel converter for wind energy storage applications. IEEE Trans Ind Electron 64(11):8867–8876
48. Eltamaly AM, Mohamed YS, El-Sayed A-HM, Elghaffar ANA (2019) Analyzing of wind distributed generation configuration in active distribution network. In: 2019 8th international conference on modeling simulation and applied optimization (ICMSAO). IEEE, pp 1–5

49. Allik A, Märss M, Uiga J, Annuk A (2016) Optimization of the inverter size for grid-connected residential wind energy systems with peak shaving. Renew Energy 99:1116–1125
50. Bawah U, Addoweesh KE, Eltamaly AM (2013) Comparative study of economic viability of rural electrification using renewable energy resources versus diesel generator option in Saudi Arabia. J Renew Sustain Energy 5(4):042701
51. Farh HM, Eltamaly AM (2013) Fuzzy logic control of wind energy conversion system. J Renew Sustain Energy 5(2):023125
52. Eltamaly AM, Farh HM (2013) Maximum power extraction from wind energy system based on fuzzy logic control. Electr Power Syst Res 97:144–150
53. Alhmoud L, Wang B (2018) A review of the state-of-the-art in wind-energy reliability analysis. Renew Sustain Energy Rev 81:1643–1651
54. Bawah U, Addoweesh KE, Eltamaly AM (2012) Economic modeling of site-specific optimum wind turbine for electrification studies. Adv Mater Res 347:1973–1986. Trans Tech Publications Ltd.
55. Eltamaly AM, Farh HM (2015) Smart maximum power extraction for wind energy systems. In: 2015 IEEE international conference on smart energy grid engineering (SEGE). IEEE, pp 1–6
56. Eltamaly AM, Alolah AI, Farh HM, Arman H (2013) Maximum power extraction from utility-interfaced wind turbines. In: New developments in renewable energy. Intech, pp 159–192
57. Tran CH, Nollet F, Essounbouli N, Hamzaoui A (2018) Maximum power point tracking techniques for wind energy systems using three levels boost converter. In: IOP conference series: earth and environmental science, vol 154, no 1. IOP Publishing, p 012016
58. Al-Shamma'a A, Addoweesh KE, Eltamaly A (2012) Optimum wind turbine site matching for three locations in Saudi Arabia. Adv Mater Res 347:2130–2139. Trans Tech Publications Ltd.
59. Wang Q, Chang L (2004) An intelligent maximum power extraction algorithm for inverter-based variable speed wind turbine systems. IEEE Trans Power Electron 19(5):1242–1249
60. Eltamaly AM, Khan AA (2011) Investigation of DC link capacitor failures in DFIG based wind energy conversion system. Trends Electr Eng 1(1):12–21
61. Li H, Shi KL, McLaren PG (2005) Neural-network-based sensorless maximum wind energy capture with compensated power coefficient. IEEE Trans Ind Appl 41(6):1548–1556
62. Al-Saud M, Eltamaly AM, Mohamed MA, Kavousi-Fard A (2019) An intelligent data-driven model to secure intravehicle communications based on machine learning. IEEE Trans Ind Electron 67(6):5112–5119
63. Eltamaly AM, Alolah AI, Abdel-Rahman MH (2011) Improved simulation strategy for DFIG in wind energy applications. Int Rev Model Simul 4(2)
64. Abir A, Mehdi D (2017) Control of permanent-magnet generators applied to variable-speed wind-energy. In: 2017 international conference on green energy conversion systems (GECS). IEEE, pp 1–6
65. Song S-H, Kang S, Hahm N (2003) Implementation and control of grid connected AC-DC-AC power converter for variable speed wind energy conversion system. In: Eighteenth annual IEEE applied power electronics conference and exposition, APEC'03, vol 1. IEEE, pp 154–158
66. Eltamaly AM (2007) Modeling of wind turbine driving permanent magnet generator with maximum power point tracking system. J King Saud Univ Eng Sci 19(2):223–236
67. Eltamaly AM, Alolah AI, Abdel-Rahman MH (2010) Modified DFIG control strategy for wind energy applications. In: Proceedings of SPEEDAM 2010. IEEE, pp 653–658
68. Mohamed MA, Eltamaly AM, Alolah AI (2017) Swarm intelligence-based optimization of grid-dependent hybrid renewable energy systems. Renew Sustain Energy Rev 77:515–524
69. Yao X, Guo C, Xing Z, Li Y, Liu S (2009) Variable speed wind turbine maximum power extraction based on fuzzy logic control. In: 2009 international conference on intelligent human-machine systems and cybernetics, vol 2. IEEE, pp 202–205
70. Eltamaly AM, Mohamed MA, Al-Saud MS, Alolah AI (2017) Load management as a smart grid concept for sizing and designing of hybrid renewable energy systems. Eng Optim 49(10):1813–1828

71. Abo-Khalil AG, Lee DC, Seok JK (2004) Variable speed wind power generation system based on fuzzy logic control for maximum output power tracking. In: Proceedings of power electronics specialists conference '04, pp 2039–2043
72. Farh HM, Eltamaly AM, Mohamed MA (2012) Wind energy assessment for five locations in Saudi Arabia. In: International conference on future environment and energy (ICFEE 2012), IPCBEE (2012) © (2012). IACSIT Press, 26–28 Feb 2012, Singapore
73. Etamaly AM, Mohamed MA, Alolah AI (2015) A smart technique for optimization and simulation of hybrid photovoltaic/wind/diesel/battery energy systems. In: 2015 IEEE international conference on smart energy grid engineering (SEGE). IEEE, pp 1–6
74. Abo-Khalil AG, Alghamdi AS, Eltamaly AM, Al-Saud MS, Praveen PR, Sayed K (2019) Design of state feedback current controller for fast synchronization of DFIG in wind power generation systems. Energies 12(12):2427
75. Alsalloum A, Hamouda RM, Alolah AI, Eltamaly AM (2010) Transient performance of an isolated induction generator under unbalanced loading conditions. J Energy Power Eng 4(5)
76. Abokhalil AG (2019) Grid connection control of DFIG for variable speed wind turbines under turbulent conditions. Int J Renew Energy Res (IJRER) 9(3):1260–1271
77. Abo-KhalilAG (2012) Synchronization of DFIG output voltage to utility grid in wind power system. Elsevier J Renew Energy 44:193–198. Impact Factor: 4.37. Abo-Khalil AG, Lee DC (2008) DC-link capacitance estimation in AC/DC/ACPWM converters using voltage injection. IEEE Trans Ind Appl 44(5). Impact Factor: 3.347
78. Abo-Khalil AG et al (2016) A low-cost PMSG topology and control strategy for small-scale wind power generation systems. Int J Eng Sci Res Technol IJESRT 585–592
79. Khaled U, Eltamaly AM, Beroual A (2017) Optimal power flow using particle swarm optimization of renewable hybrid distributed generation. Energies 10(7):1013
80. Abo-KhalilAG (2013) Impacts of wind farms on power system stability. Wind farm. ISBN 980-953-307-562-9
81. El-Tamaly HH, El-Tamaly AM, El-Baset Mohammed AA (2003) Design and control strategy of utility interfaced PV/WTG hybrid system. In: The ninth international middle east power system conference, MEPCON, pp 16–18
82. Abo-Khalil AG (2011) A new wind turbine simulator using a squirrel-cage motor for wind power generation systems. In: The power electronics and drive systems conference PEDS, Dec 2011, Singapore
83. Eltamaly AM (2012) A novel harmonic reduction technique for controlled converter by third harmonic current injection. Electr Power Syst Res 91:104–112
84. Park HG, Abo-Khalil AG, Lee DC, Son KM (2007) Torque ripple elimination for doubly-fed induction motors under unbalanced source voltage. In: Proceedings of power electronics and drive systems PEDS'07, Nov 2007, pp 1301–1306
85. Eltamaly AM, Al-Shamma'a AA (2016) Optimal configuration for isolated hybrid renewable energy systems. J Renew Sustain Energy 8(4):045502
86. Abo-Khalil AG, Lee DC (2006) Dynamic modeling and control of wind turbines for grid-connected wind generation system. In: Proceedings on power electronics specialists conference, Korea
87. Eltamaly AM (2009) Harmonics reduction techniques in renewable energy interfacing converters. Renew Energy. Intechweb
88. Abo-Khalil AG, Lee DC (2006) Grid connection of doubly-fed induction generators in wind energy conversion. In: Proceedings of IPEMC, China, Aug 2006
89. Eltamaly AM (2000) Power quality consideration for interconnecting renewable energy power converter systems to electric utility. PhD diss, PhD thesis, Elminia University